Laser irradiation induced tunable localized surface plasmon resonance of silver thin film

Ruijin Hong [a, b], Wen Shao [a], Wenfeng Sun [a], Cao Deng [a], Chunxian Tao [a], Dawei Zhang [a, *]

[a] Engineering Research Center of Optical Instrument and System, Ministry of Education and Shanghai Key Lab of Modern Optical System, University of Shanghai for Science and Technology, No.516 Jungong Road, Shanghai, 200093, China
[b] State Key Laboratory of Applied Optics, Changchun Institute of Optics, Fine Mechanics and Physics, Chinese Academy of Sciences, Changchun, 130033, China

ARTICLE INFO

ABSTRACT

Tunable localized surface plasmon resonance (LSPR) properties of silver thin films were realized by CO_2 laser irradiation. The effects of laser irradiation on the structure, morphology and optical property of the samples were investigated by X-ray diffraction (XRD), scanning electron microscope (SEM), atomic force microscopy (AFM), UV-VIS-NIR double beam spectrometer and Raman system, respectively. XRD patterns show that laser irradiation has the effects of improving grain growth and orientation of Ag thin films. With laser irradiation power increasing, the topography of as-irradiated silver thin films were observed to develop discontinuous nano-ellipsoid structure with a red-shift of the surface plasmon resonance wavelength in visible region. Both the various ellipsoid sizes and the states of aggregation of as-irradiated silver thin films contributed to increase significantly the sensitivity of surface enhanced Raman scattering (SERS). Additionally, the simulation result of Finite-Difference Time-Domain (FDTD) was proved to be in good agreement with that of the experiment.

© 2018 Elsevier B.V. All rights reserved.

1. Introduction

Surface plasmons have attracted lots of interests in recent years for their localized surface plasmon resonance (LSPR) properties [1,2]. When the resonance frequency of conduction electrons and incident light are matched, LSPR induced by collective electron charge oscillations in metallic nanoparticles (NPs) shows its strong confinement and enhancement of near-field amplitude [3–5]. It is indicated that LSPR has many potential applications, such as surface enhanced Raman scattering (SERS) [6,7], photothermal therapy [8,9], nonlinear optics [10], biological and chemical sensors [11–13], plasmon enhanced fluorescence [14,15] and other fields. In particular, SERS has attracted considerable attention due to its nondestructive and single molecular level sensitivity [16–18]. The efficiency and intensity of these applications largely depend on the LSPR wavelength which is not only determined by the size, shape and the surrounding medium of metallic NPs but also by metal materials [4,19–21]. It is demonstrated that strong tunable LSPR can be achieved by modifying these factors appropriately.

At present, researches on surface plasmon resonance mainly focus on noble metals which have the unique LSPR properties due to their strong resonant oscillations [2,9,22]. Among various noble metals, silver, gold and copper are mostly used in plasmonic applications because of their low optical loss. Gold has the advantage of being chemically stable but a higher cost compared with silver. Considering the cost of silver and gold, copper is applicable yet it is easily oxidized [23]. Therefore, silver (Ag) is a reasonable choice to research LSPR properties. Its fine LSPR tunability from visible to near-infrared wavelength can be realized by controlling the size and shapes of Ag NPs appropriately. However, it is still a challenge to fabricate desirable size and shapes of Ag NPs. For examples, electron beam irradiation technique shows slow and costly processes [24]; the arrangement of colloid monolayers has disadvantages about poor reproducibility [25]. Compared to these conventional methods, laser irradiation technique has been studied theoretically and experimentally for its unique advantages which make Ag thin films transformed into droplets with different shapes directly due to its good ductility [26,27]. These Ag samples with nanoparticle structures can be fast and easily prepared by this technique with flexible and low-cost process at the same time. To achieve the tunable LSPR properties, laser irradiation technique is
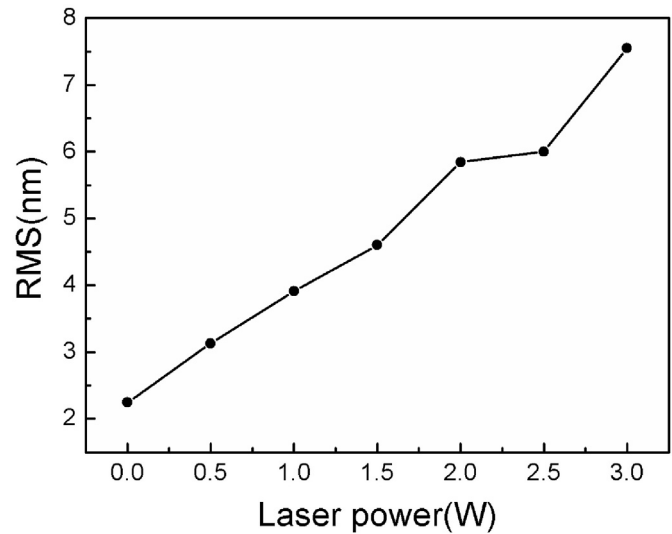
* Corresponding author.
  E-mail address: dwzhang@usst.edu.cn (D. Zhang).
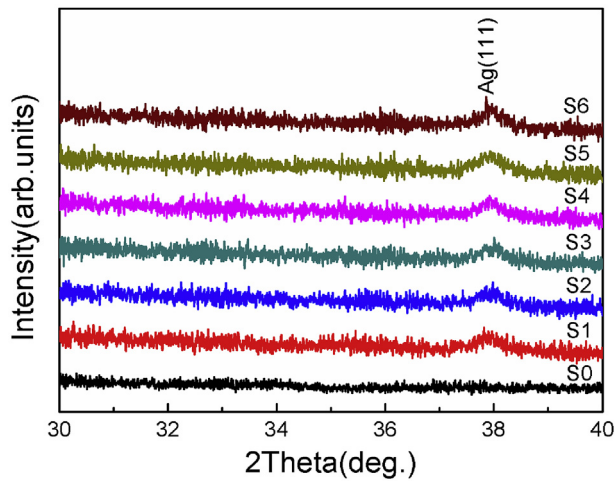
Fig. 1. The XRD patterns of the as-annealed and as-irradiated Ag thin films with various laser powers.

Fig. 3. Surface roughness of Ag thin films corresponding to gradually increased laser power.

applied to prepare Ag NPs with various sizes and gaps by changing certain parameters of the laser equipment such as laser wavelength, laser energy and scan rate and so on. Nevertheless, the practical application of laser irradiation technique is still worthy of deeper researches for its detailed influence on the sizes and shapes of NPs.

In this paper, we proposed a cost-effective technique, CO_2 laser irradiation, to achieve fine LSPR tunability of Ag thin film. This CO_2 laser with long wavelength, different from the short-wave lasers which are commonly used to prepare Ag NPs in previous experiments, only has the thermal transmission when irradiates Ag thin films. The LSPR absorption peaks of the Ag thin films were tuned by varying the laser irradiation power. The influences of laser irradiation power on the structure, optical absorption and Raman scattering properties of Ag thin films were investigated in the paper.

Also, the simulation method of Finite-Difference Time-Domain (FDTD) was employed to figure out the electric field distribution of Ag thin films.

2. Experiment

Ag thin films with a thickness of 15 nm were deposited on fused quartz substrates by electron beam evaporation at room temperature. The thickness of thin films was monitored by a quartz crystal microbalance. After finishing the deposition process, the as-deposited thin films were annealed in situ in the same vacuum chamber with the temperatures of 100 °C for 30 min. These as-annealed Ag thin films were irradiated by a continuous wave CO_2
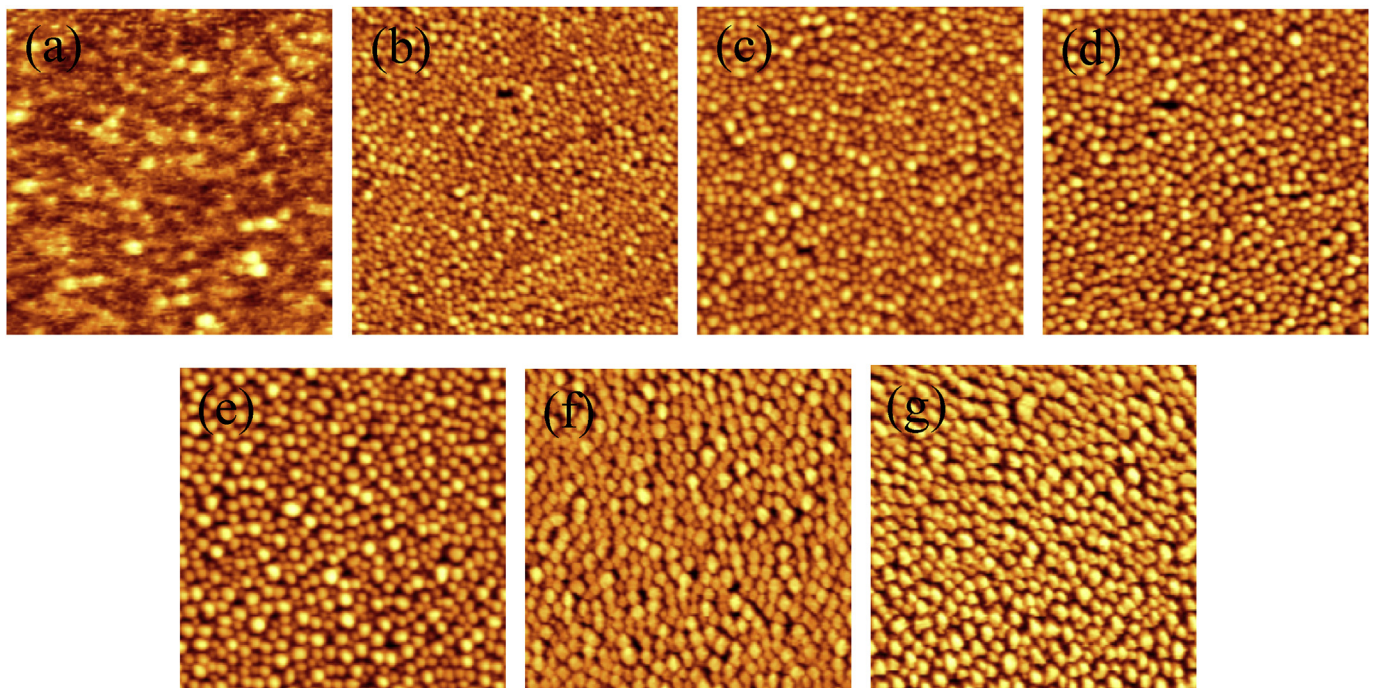
Fig. 2. AFM images of Ag thin films irradiated with laser powers of (a) 0 W, (b) 0.5 W, (c) 1 W, (d) 1.5 W, (e) 2 W, (f) 2.5 W and (g) 3 W.
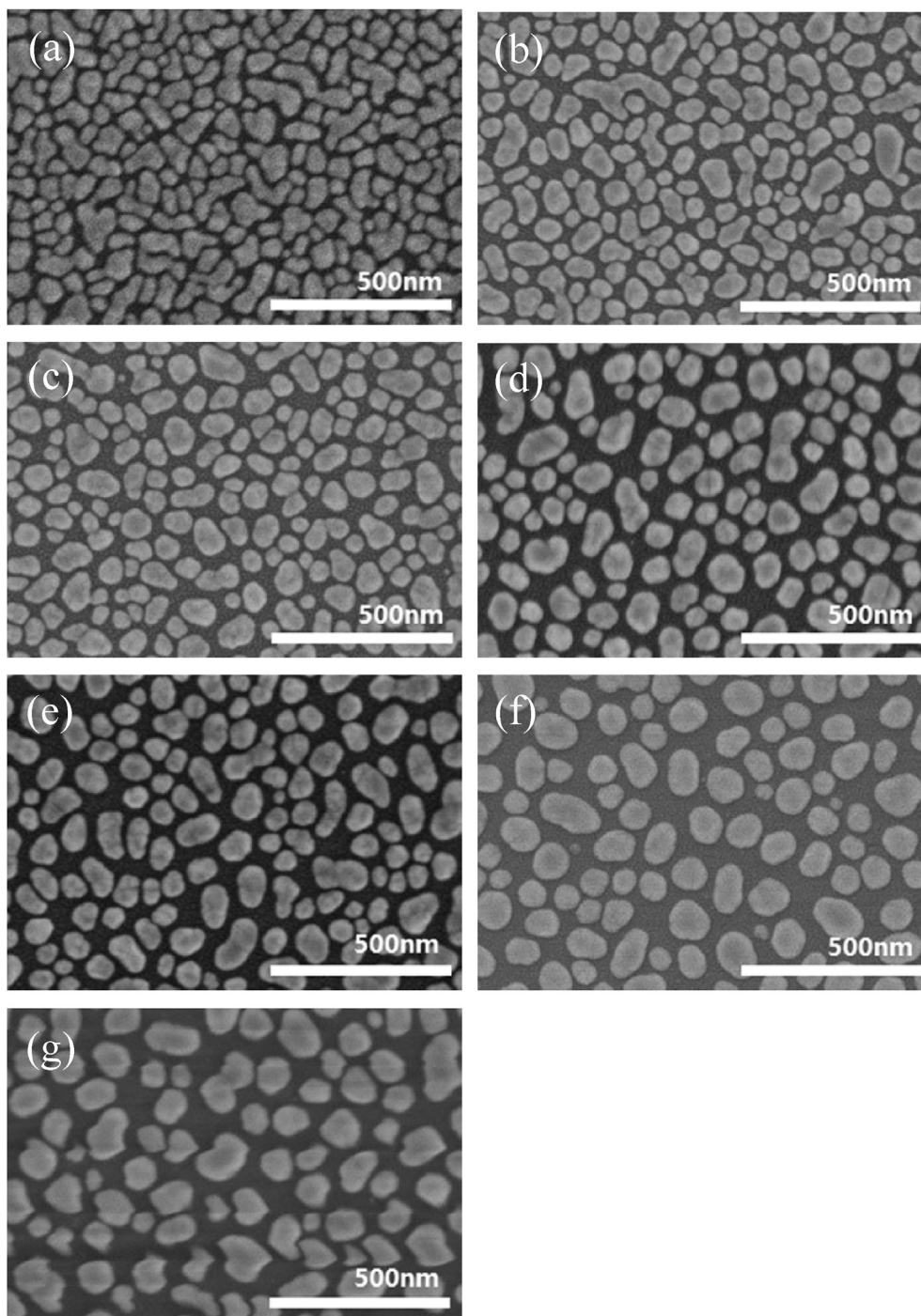
Fig. 4. SEM images of Ag thin films with laser powers of (a) 0 W, (b) 0.5 W, (c) 1 W, (d) 1.5 W, (e) 2 W, (f) 2.5 W and (g) 3 W.

laser source whose wavelength is 10.6 μm with various laser powers. The laser parameters adopted in the experiment were as follow: laser beam powers were set as 0.5, 1, 1.5, 2, 2.5 and 3 W, respectively, the beam diameter was 0.1 mm, and the scan speed was set as 50 mm/s. For comparison, as-annealed Ag thin film was also used in the study. The as-annealed film and as-irradiated films were marked as sample 0 (S0), sample 1 (S1), sample 2 (S2), sample 3 (S3), sample 4 (S4), sample 5 (S5) and sample 6 (S6), respectively, which are in accord with the increasing laser power (0−3 W).

The crystal structure of the samples were analyzed by X-ray diffraction (XRD) using a Rigaku MiniFlex600 system, with Cu Kα

radiation (λ = 0.15408 nm). The surface morphology and roughness were characterized by atomic force microscopy (AFM) (XE-100, Park System) and scanning electron microscope (SEM) (S-4800, Hitachi). The optical absorption of the samples was measured with an UV-VIS-NIR double beam spectrophotometer (Lambda 1050, Perkins Elmer), the scan step and integration time were set 2 nm and 0.24 s, respectively. Raman scattering spectra were examined using a confocal microprobe Raman system (inVia Raman Microscope, Renishaw) with 633 nm laser. All the measurements were carried out at room temperature.
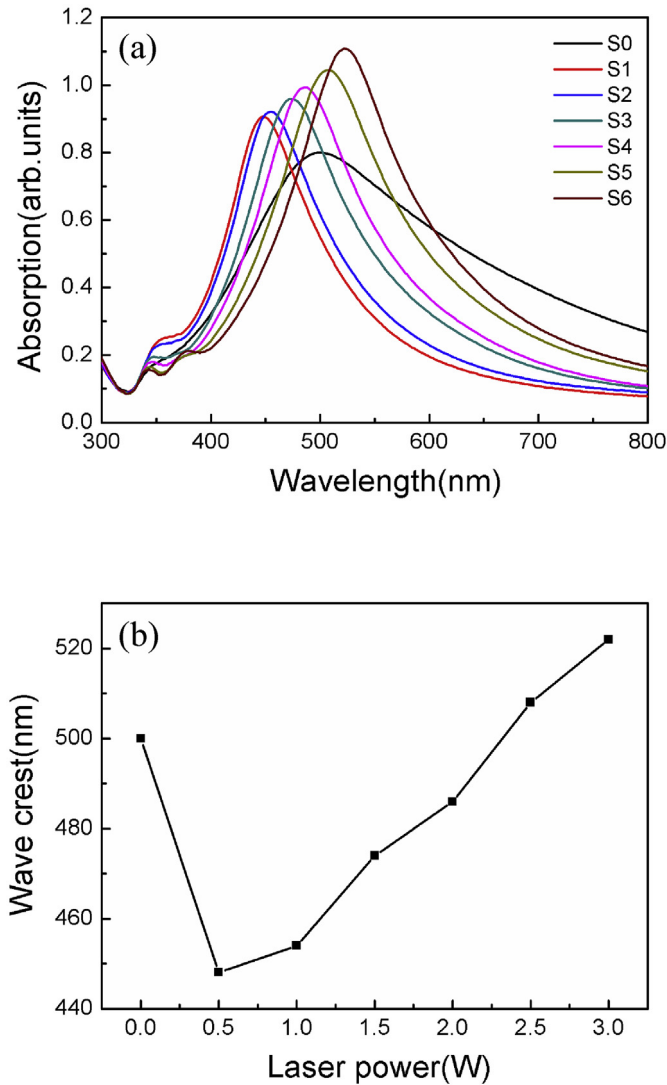
Fig. 5. (a) Absorption spectra of Ag thin films with increased laser irradiated powers; (b) Curve of wave crests from every absorption spectrum.
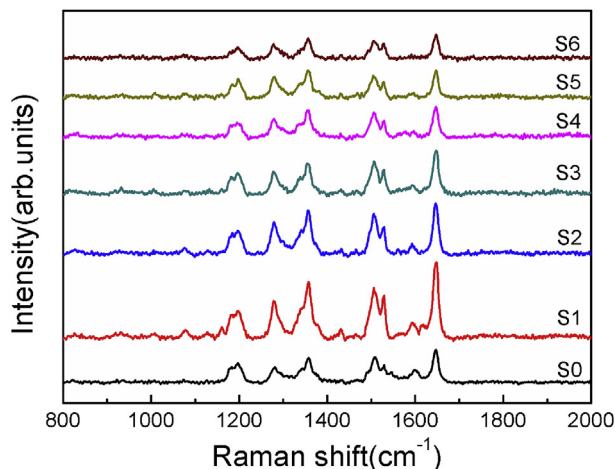
Fig. 6. Raman scattering spectra of Rh B on Ag thin films with increasing laser powers.

3. Results and discussion

3.1. Structural properties

The XRD patterns as shown in Fig. 1 reveal the influence of laser irradiation on the structure of Ag thin films. According to Fig. 1, no diffraction peaks are observed in the as-annealed sample, meaning that it is amorphous. However, a broad diffraction peak appears in the as-irradiated samples at around 38.184° (2θ), which is corresponding to (111) crystallographic plane (JCPDS: 04—0783). It indicates that no obvious grain growth is observed during the case of annealing processing, while the grain growth occurs by laser irradiation. Additionally, the intensity of the diffraction peaks has a slight increase with the laser power increasing. It also indicates the preferential orientation of Ag grains along the (111) crystallographic direction. The results show that laser irradiation leads to the occurrence of (111) crystallographic direction of lowest surface energy and improves the crystallinity of Ag thin films.

3.2. Surface morphology

Fig. 2 shows the AFM images with the scanning area of 3 μm × 3 μm for as-annealed sample (Fig. 2 (a)) and as-irradiated samples (Fig. 2 (b)-(g)). The morphology of as-annealed sample exhibits disorder (as shown in Fig. 2 (a)). After being modified by laser irradiation, the thin film was transformed into orderly spheroidal structure. According to Fig. 2 (b)-(g), the size and spacing of those structured samples increase with the increase of laser powers. The values of the root mean square (RMS) surface roughness of these samples are 2.244, 3.131, 3.911, 4.601, 5.846, 6.000 and 7.552 nm, respectively, as shown in Fig. 3.

Fig. 4 shows the SEM images of Ag thin films with various laser powers. In Fig. 4 (a), the as-annealed sample shows a disorder surface. It is obvious that laser irradiation makes Ag thin films broken into defined particles with a discontinuous structure according to Fig. 4 (b)-(g). With the laser power increasing, Ag NPs with nano-ellipsoid structure have the gradually increasing particle size and spacing. These SEM results illustrate the uniformity with AFM images.

In case of laser irradiation, the laser energy is transferred to Ag thin films, resulting in the thin film melts. Then instability of the films drives breakup into droplets with nanosize solid metallic particles since Ag is among the metals that poorly wet the substrate. This breakup allows the self-assembly of supported nanoparticle arrays therefore Ag thin films are readily transformed into Ag NPs with nano-ellipsoid structure by laser irradiation [27,28]. With the increase of laser power, the size of Ag NPs becomes lager, which results in the increase of the distances between particles. Additionally, the grain growth means the higher grain size, broadened height distribution and low valleys, which causes the increase of RMS [29].

3.3. Optical absorption

Fig. 5 (a) shows the absorption spectra of as-annealed and as-irradiated Ag thin films. For as-annealed sample, the shape of its absorption spectrum which is similar to those reported by others [30], is featured by a broad peak at about 500 nm. However, for the as-irradiated sample, the resonance absorption shifts to the shorter wavelength with a narrowed peak. Along with the increasing laser powers, there is a red-shift of LSPR wavelength from 448 to 522 nm and a rise of absorption intensity in the absorption spectra of as-irradiated samples. As shown in Fig. 5 (b), there is a wave crest which represents the wavelength corresponding to the maximum absorption in each absorption spectrum, and the value of these
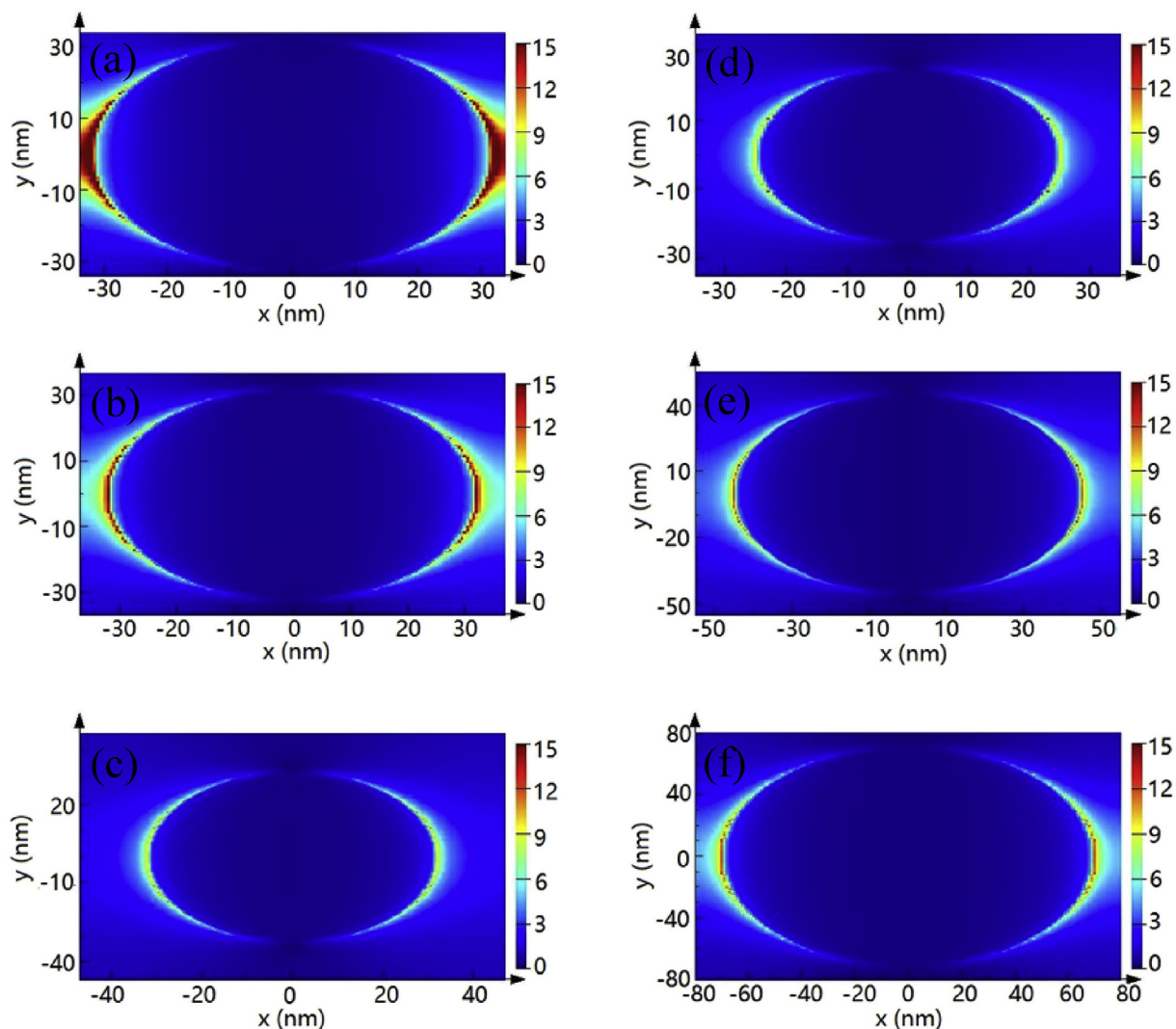
Fig. 7. FDTD simulated electric field amplitude patterns for Ag NPs (a)–(c) with the same particle radius but increasing gaps and (d)–(f) with the same particle gaps but increasing radius.

wavelengths is 500, 448, 454, 474, 486, 508 and 522 nm, respectively.

It is apparent that laser irradiation has the modified effect on the shift of LSPR wavelength and the intensity of absorption peak by varying the laser power. This phenomenon can be explained by the surface morphology of Ag thin films, as shown in SEM images (Fig. 4 (a)-(g)). By laser irradiation, the Ag thin film is transformed into nano-ellipsoid structure which enables the existence of stronger LSPR [29], and the discontinuity of Ag thin film produces a stronger resonant frequency which results in the blue-shift between as-annealed and as-irradiated samples (S0 and S1). At the same time, the continuous thin film with a broad peak develops into structured ellipsoid that leads to the existence of a narrowed peak [4]. During laser irradiation, the thermal energy from CO_2 laser is transferred into Ag thin films, resulting in the different size and spacing of Ag NPs with different laser powers. The plasmon wavelength and absorption cross-sections vary with the size and shape of the NPs, according to the Gans theory, the popular qua-sistatic theory about the calculation for the optical absorption of NPs with an ellipsoidal structure [31]. The plasmon wavelength nearly linearly relies on the diameter of the NPs, therefore the LSPR wavelength red-shifts due to the increased size of Ag NPs. On the other hand, the enhanced intensity of LSPR peak is attributed to the higher absorption cross section of the lager particles size [24]. It indicates that the oscillation modes have direct relations to the size of Ag NPs, and that the plasmon absorption maximum shifts to longer wavelength with the size of Ag NPs increasing [32]. In general, laser irradiation directly causes the shift of the plasma resonant peak.

3.4. SERS performance

To research the potential application of LSPR properties, these samples were used as SERS substrates in the experiment. The probing Rhodamine B (Rh B) molecule which is a typical artificial dye was chosen as a test compound to study the application of Ag thin films. The Rh B molecule solutions with the concentration of 10^{-4} mol/L were dosed onto the surface of these Ag samples. In Fig. 6, the three strongest Raman peaks, at about 1648, 1361 and 1504 cm^{-1}, corresponding to C=C stretching modes of aromatic rings are observed in the as-annealed sample. With low power laser irradiation, the Raman scattering intensity of Rh B molecule significantly enhances on the as-irradiated substrates. However, the Raman signal intensities gradually decrease with the irradiated

laser powers further increasing. It is apparent that the Raman signal intensities of as-irradiated samples can be adjusted flexibly in accord with the different laser powers.

On the basis of the electromagnetic enhancement theory, by laser irradiation, the surfaces of samples are rougher and more structured, but the size and the gap of Ag NPs become lager, which causes less tips or "hot spots" to excite the local electrical fields, resulting in the decrease of Raman intensity [33]. As a result, the increasing laser power easily modifies the size and spacing of Ag NPs and on this account it controls the intensity of Raman signals as well.

To further verify the conclusions above, the simulation of Finite-difference time domain (FDTD) was employed to calculate the electric field distribution for these laser irradiated samples. In this simulation, a 633 nm laser irradiated perpendicularly to the x-y plane of the Ag samples with the polarization along the y-axis direction. Fig. 7 illustrates the electric field intensity of Ag NPs with various sizes and gaps. For these Ag NPs with the same size in radius and different particle gaps (Fig. 7 (a)-(c)), the intensity of the electric field has a decreased trend when the gap becomes lager. The tips or "hot spots", gather of the red spots on local surface in figures, formed between the spacing of NPs tend to be obviously weaker from Fig. 7 (a) to (c) due to the increasing gaps. Furthermore, in order to prove the particle spacing is more influential than particle size on electric field intensity, Ag NPs with the same particle gaps and increasing sizes are shown in Fig. 7 (d)-(f). It demonstrates that when the particle sizes become lager, the electric field intensity in Ag NPs has no significant difference if there exists enough distance between particles. On the whole, the increase of gaps in Ag NPs leads to the decrease of the SERS intensity due to the weak intensity of tips or "hot spots". The simulation results are in good agreement with the experimental results above.

4. Conclusions

In conclusion, the influences of laser irradiation on Ag thin films for structural and optical properties were investigated in this paper. The results show that laser irradiation can improve the grain growth and orientation of Ag thin films and transforms the thin films into nano-ellipsoid structures. The LSPR wavelength red-shifts in visible region for the increasing size and spacing of Ag NPs induced by various laser powers. Additionally, the Raman scattering can be adjusted by different laser power due to the variation of LSPR in Ag NPs, which is in line with the results of FDTD simulation.

References

[1] W.L. Barnes, A. Dereux, T.W. Ebbesen, Surface plasmon subwavelength optics, Nature 424 (2003) 824–830.
[2] E. Hutter, J.H. Fendler, Exploitation of localized surface plasmon resonance, Adv. Mater. 16 (2004) 1685–1706.
[3] T.K. Sau, A.L. Rogach, F. Jäckel, T.A. Klar, J. Feldmann, Properties and applications of colloidal nonspherical noble metal nanoparticles, Adv. Mater. 22 (2010) 1805–1825.
[4] K.L. Kelly, E. Coronado, L.L. Zhao, G.C. Schatz, The optical properties of metal nanoparticles: the influence of size, shape, and dielectric environment, J. Phys. Chem. B 107 (2003) 668–677.
[5] S. Verma, B.T. Rao, A.P. Detty, V. Ganesan, D.M. Phase, S.K. Rai, A. Bose, S.C. Joshi, L.M. Kukreja, Surface plasmon resonances of Ag-Au alloy nano-particle films grown by sequential pulsed laser deposition at different compositions and temperatures, J. Appl. Phys. 117 (2015) 205.
[6] H.-Y. Wu, C.J. Choi, B.T. Cunningham, Plasmonic nanogap-enhanced Raman scattering using a resonant nanodome array, Small 8 (2012) 2878.
[7] C. Zhu, G. Meng, Q. Huang, Z. Zhang, Q. Xu, G. Liu, Z. Huang, Z. Chua, Ag nanosheet-assembled micro-hemispheres as effective SERS substrates, Chem. Commn. 47 (2011) 2709–2711.
[8] J. Song, P. Huang, H. Duan, X. Chen, Plasmonic vesicles of amphiphilic nano-crystals: optically active multifunctional platform for cancer diagnosis and therapy, Acc. Chem. Res. 48 (2015) 2506–2515.
[9] L.A. Austin, M.A. Mackey, E.C. Dreaden, M.A. El-Sayed, The optical, photo-thermal, and facile surface chemical properties of gold and silver nano-particles in biodiagnostics, therapy, and drug delivery, Arch. Toxicol. 88 (2014) 1391–1417.
[10] P. Muhlschlegel, H.-J. Eisler, O.J.F. Martin, B. Hecht, D.W. Pohl, Resonant otical atennas, Science 308 (2005) 1607–1609.
[11] K. Shrivas, R. Shankar, K. Dewangan, Gold nanoparticles as a localized surface plasmon resonance based chemical sensor for on-site colorimetric detection of arsenic in water samples, Sens, Actuators B 220 (2015) 1376–1383.
[12] M. Hu, J. Chen, Z.Y. Li, L. Au, G.V. Hartland, X. Li, M. Marquez, Y. Xia, Gold nanostructures: engineering their plasmonic properties for biomedical applications, Chem. Soc. Rev. 35 (2006) 1084–1094.
[13] A.V. Kabashin, P. Evans, S. Pastkovsky, W. Hendren, G.A. Wurtz, R. Atkinson, R. Pollard, V.A. Podolskiy, A.V. Zayats, Plasmonic nanorod metamaterials for biosensing, Nature Mater. 8 (2009) 867–871.
[14] J.R. Lakowicz, Radiative decay engineering 5: metal-enhanced fluorescence and plasmon emission, Anal. Biochem. 15 (2005) 171–194.
[15] F. Xie, A. Centeno, M.R. Ryan, D.J. Riley, N.M. Alford, Au nanostructures by colloidal lithography: from quenching to extensive fluorescence enhancement, J. Mater. Chem. B 1 (2012) 536–543.
[16] H. Im, K.C. Bantz, S.H. Lee, T.W. Johnson, C.L. Haynes, S.H. Oh, Self-assembled plasmonic nanoring cavity arrays for SERS and LSPR biosensing, Adv. Mater. 25 (2013) 2677.
[17] K.A. Willets, R.P.V. Duyne, Localized surface plasmon resonance spectroscopy and sensing, Annu. Rev. Phys. Chem. 58 (2007) 267–297.
[18] T. Tan, C. Tian, Z. Ren, J. Yang, Y. Chen, L. Sun, Z. Li, A. Wu, J. Yin, H. Fu, LSPR-dependent SERS performance of silver nanoplates with highly stable and broad tunable LSPRs prepared through an improved seed-mediated strategy, Phys. Chem. Chem. Phys. 15 (2013) 21034–21042.
[19] P.K. Jain, M.A. El-Sayed, Plasmonic coupling in noble metal nanostructures, Chem. Phys. Lett. 487 (2010) 153–164.
[20] P. Mulvaney, Surface plasmon spectroscopy of nanosized metal particles, Langmuir 12 (1996) 788–800.
[21] S.Y. Gezgin, H.Ş. Kılıç, A. Kepceoğlu, S. Bayır, İ.E. Nalbantoğlu, A. Toprak, Plasmonic tuning of gold doped thin films for layers of photovoltaic devices, AIP Conf. Proc. 1722 (2016) 3806–3819.
[22] A.R. Tao, S. Habas, P. Yang, Shape control of colloidal metal nanocrystals, Small 4 (2008) 310–325.
[23] P.R. West, S. Ishii, G.V. Naik, N.K. Emani, V.M. Shalaev, A. Boltasseva, Searching for better plasmonic materials, Laser Photonics Rev. 4 (2010) 795–808.
[24] R.G. Nikov, N.N. Nedyalkov, P.A. Atanasov, D. Hirsch, B. Rauschenbach, K. Grochowska, G. Sliwinski, Characterization of Ag nanostructures fabricated by laser-induced dewetting of thin films, Appl. Surf. Sci. 374 (2016) 36–41.
[25] T. Okamoto, I. Yamaguchi, T. Kobayashi, Local plasmon sensor with gold colloid monolayers deposited upon glass substrates, Opt. Lett. 25 (2000) 372–374.
[26] M. Ullmann, S.K. Friedlander, A. Schmidt-Ott, Nanoparticle formation by laser ablation, J. Nanopart. Res. 4 (2002) 499–509.
[27] S.J. Henley, J.D. Carey, S.R.P. Silva, Pulsed-laser-induced nanoscale island formation in thin metal-on-oxide films, Phys. Rev. B 72 (2005) 195408.
[28] F. Mafune, J. Kohno, A. Yoshihiro Takeda, T. Kondow, H. Sawabe, Formation and size control of silver nanoparticles by laser ablation in aqueous solution, J. Phys. Chem. B 104 (2000) 9111–9117.
[29] W. Wei, R. Hong, Y. Meng, C. Tao, D. Zhang, Electron-beam irradiation induced phase transformation, optical absorption and surface-enhanced Raman scattering of Indium tin alloy thin films, Superlattices Microstruct. 106 (2017) 189–196.
[30] Y. Fang, L. Hong, L. Wan, K. Zhang, X. Lu, C. Wang, Localized surface plasmon of Ag nanoparticles affected by annealing and its coupling with the excitons of Rhodamine 6G, J. Vac. Sci. Technol. A 31 (2013) 041401-041401-5.
[31] H. Chen, L. Shao, Q. Li, J. Wang, Gold nanorods and their plasmonic properties, Chem. Soc. Rev. 42 (2013) 2679–2724.
[32] S. Link, M.A. El-Sayed, Size and temperature dependence of the plasmon absorption of colloidal gold nanoparticles, J. Phys. Chem. B 103 (1999) 4212–4217.
[33] M. Fan, A.G. Brolo, Silver nanoparticles self-assembly as SERS substrates with near single molecule detection limit, Phys. Chem. Chem. Phys. 11 (2009) 7381–7389.